

Conf-760202--20

HEALTH PHYSICS SOCIETY
Ninth Midyear Topical Symposium

Part of this article, the publisher or
author reserves the right to make it
available - exclusive, royalty-free
and to any copyright covering the

DETECTION OF INTERNALLY DEPOSITED ACTINIDES
PART IV: PRELIMINARY CONSIDERATIONS
IN THE USE OF LARGE, PLANAR INTRINSIC GE DETECTORS *

C. E. Semis, Jr., R. E. Goans, W. M. Good and G. G. Warner
Oak Ridge National Laboratory
Oak Ridge, Tennessee 37830

Abstract

Many inherent advantages are apparent in the use of large planar Ge detectors for the detection, identification and quantitative assessment of internally deposited actinide nuclides. The superior energy resolution in contrast to "Phoswich type" scintillation detectors, permits isotopic identifications to be made and reduces ambiguities introduced by natural and human background effects. Our preliminary studies indicate that a $10 \text{ cm}^2 \times 1.2 \text{ cm}$ Ge detector is comparable in detection sensitivity to that of one 125 cm^2 "Phoswich" detector. Some preliminary considerations and evaluations, photon transport studies based on Monte Carlo modeling and measurements of absolute L-series X-ray yields in the decay of several actinide nuclides, are presented.

Introduction

The impact of silicon and germanium semiconductor detectors for the measurement of low energy photons has been tremendous since their introduction over a decade ago. Basic research efforts in nuclear, atomic and solid state physics, in geological and extraterrestrial studies and other disciplines have all benefited by the use of these detectors. They are used routinely in environmental monitoring, oil well logging, in activation analysis and in safeguards applications to name a few and to some extent, in applied health physics applications. In the photon energy domain of $\sim 150 \text{ keV}$ to 2 MeV and higher, it is quite clear that conventional semiconductor photon spectrometers will never attain the detection efficiency realized by the use of CsI or NaI scintillation spectrometers. However, the energy resolution enhancement offered by Ge semiconductor detectors more than offsets the inferior detection efficiency and in counting situations where the precision tends to be poor, the use of Ge detectors is clearly indicated.^{(1),(2)} The inherent gain stability and high resolution of semiconductor spectrometers greatly add to the practitioner's confidence in making such measurements.

In the lower photon energy domain of about $10\text{-}150 \text{ keV}$, both the Ge semiconductor and the NaI scintillation spectrometers are "black" to photons and the absolute detection efficiencies are for the most part, governed by solid angle considerations. In this energy range, the superior resolving power of Ge detectors is most evident and their use in low intensity applied health physics applications is extremely desirable. One particular health physics application that could greatly benefit is the "in-vivo" detection of respiration actinide nuclides using external detectors. This study represents some of our preliminary efforts to define and parameterize some of the variables involved in this particular application and hopefully will be of general applicability.

L-X-Ray Energies and Absolute L-Series X-Ray Yields

Most actinide nuclides of importance in applied health physics are difficult to detect "in-vivo" using external detectors because of the absence of "hard" photonic radiations in sufficient abundance to be detectable. Characteristic L-series X rays, and in a few cases low energy gamma rays, do accompany the alpha decay of these nuclides and it is usually these radiations that are detected externally. These L-series X rays, with energies in the range $10\text{-}25 \text{ keV}$, are seriously attenuated by the intervening tissue but the energy dependent attenuation can lead to an independent determination of the average soft tissue overburden in the same measurement if more than one L-X ray line is observed. Clearly, only the Ge detector is capable of providing the required energy resolution ($\sim 300\text{-}400 \text{ eV FWHM}$) as typical scintillation detectors in this low energy range have resolutions ($\Delta E/E$) of $\sim 50\%$ or $8\text{-}10 \text{ keV}$. An unattenuated curium L-X-ray spectrum arising in the decay of 13-year ^{250}Cf is shown in Figure 1 and is typical in structure with those of other actinide nuclides. Energies of the most prominent and easily identifiable L-series X rays, the L_2 , L_{21} , L_{31} and L_{41} lines for the elements $Z = 90$ thru $Z = 100$ (Th-Fm) are listed in Table 1. Nearly all semiconductor detector L-X ray spectra measured at an energy resolution better than $\sim 1 \text{ keV FWHM}$ may be partitioned into four broad groups, the L_2 , L_{21} , L_3 and L_4 groups, even though all L-series lines are not readily identifiable.

* Research sponsored by the U. S. Energy Research and Development Administration under contract with Union Carbide Corporation.

NOTICE

This report was prepared as an account of work sponsored by the United States Government. Neither the United States nor the United States Energy Research and Development Administration, nor any of their employees, nor any of their contractors, subcontractors, or their employees, makes any warranty, express or implied, or assumes any liability or responsibility for the accuracy, completeness or usefulness of any information, apparatus, product or process disclosed, or represents that its use would not infringe privately owned rights.

DISTRIBUTION OF THIS DOCUMENT IS UNLIMITED

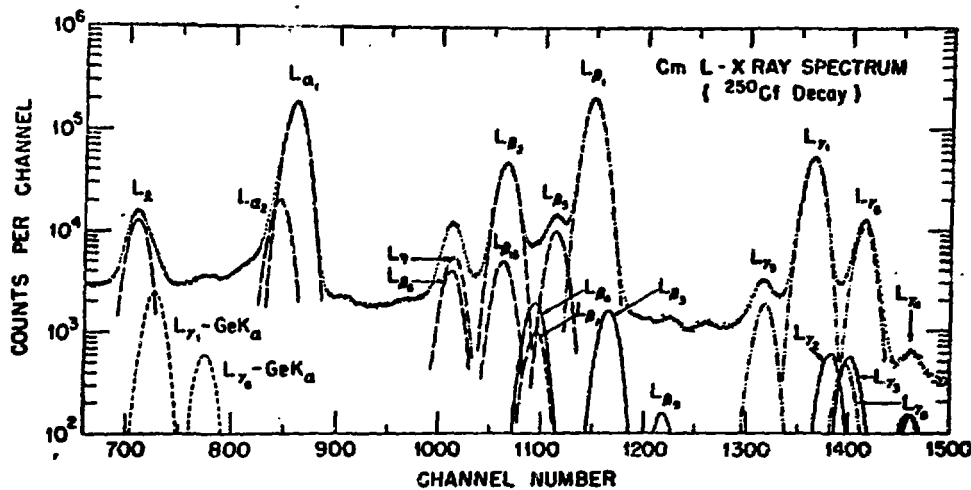


Figure 1. L-X ray spectrum of curium arising in the alpha decay of 13 year ^{250}Cf . The dashed line peaks, the dot-dash line and the solid line peaks designate lines arising from the L_3 , L_2 and L_1 shells respectively. The energy resolution is approximately 250 eV at FWHM.

Table 1. Energies in keV of Prominent L-Series X-Ray Lines for the Elements Th-Ca.

Element	Z	Line Designation			
		L_{μ}	$L_{\alpha 1}$	$L_{\beta 1}$	$L_{\gamma 1}$
Th	90	11.119	12.969	16.202	18.983
Pa	91	11.366	13.291	16.702	19.568
U	92	11.618	13.615	17.220	20.167
Kp	93	11.890	13.944	17.750	20.795
Pu	94	12.124	14.279	18.294	21.417
An	95	12.384	14.617	18.852	22.065
Cm	96	12.650	14.959	19.426	22.730
Bk	97	12.917	15.307	20.006	23.417
Cf	98	13.174	15.660	20.611	24.116
Es	99	13.429	16.014	21.234	24.835
Fm	100	13.685	16.374	21.875	25.574

To provide accurate L-series X-ray intensities, we have measured the characteristic L-X ray spectra arising in the decay of several actinide nuclides of importance in applied health physics.⁽³⁾ Isotopically pure point sources were prepared directly on thin carbon (40 $\mu\text{g}/\text{cm}^2$) or thin nickel foils (0.9 $\mu\text{g}/\text{cm}^2$) using an isotope separator. Absolute disintegration rates were established by alpha counting using standard 2 π proportional counters operated with argon-methane. The low energy photon spectra were measured using a 10 cm^2 x 1.2 cm intrinsic planar Ge detector in fixed reproducible geometries. The Ge detector efficiency calibration was established using calibrated sources of ^{241}Am , ^{57}Co , ^{103}Cd and ^{113}Sn and using the evaluated photon intensities of Campbell and McElwes.⁽⁴⁾ In order to avoid difficulties that occur close to the K-absorption edge in Ge (~11.1 keV), measurements were also made using a Si(Li) detector. These absolute intensity measurements for some of the nuclides studied are given in Table 2 for the L₁, L₂, L₃ and L₄ groups. The uncertainties in the intensities are the standard deviation and include uncertainties in source disintegration rate as well as the uncertainties in detector efficiency. Using these absolute L-X ray yields for the isotopically pure samples, yields for mixed isotopic samples, as is most often the case with the Pu isotopes, may easily be constructed. Absolute yields and energies for some of the low energy gamma ray transitions are to be included in a future report⁽³⁾ and these transitions, often much less intense than the L-X rays, can be used as an additional identification aid. Of course, the energies of the L-X rays uniquely identify the element as is evident by an inspection of Table 1.

Table 2. Absolute L-X Ray Intensities in the Decay of Several Actinide Nuclides.

Parent Nuclide	$\frac{I}{Z}$ per disintegration				
	L_L	L_a	L_B	L_γ	zL
^{238}Pu	0.26 ± 0.01	4.15 ± 0.07	3.61 ± 0.07	1.36 ± 0.02	11.38 ± 0.10
^{239}Pu	0.113 ± 0.005	1.82 ± 0.04	2.16 ± 0.04	0.53 ± 0.01	4.63 ± 0.06
^{240}Pu	0.24 ± 0.01	3.78 ± 0.06	4.84 ± 0.07	1.20 ± 0.03	10.06 ± 0.10
^{242}Pu	0.21 ± 0.02	3.10 ± 0.08	4.15 ± 0.10	1.08 ± 0.04	8.54 ± 0.14
$^{241}\text{Am}^{(a)}$	0.86 ± 0.03	13.2 ± 0.3	19.25 ± 0.60	4.85 ± 0.2	38.2 ± 0.7
^{246}Cm	0.25 ± 0.01	3.86 ± 0.07	4.30 ± 0.07	1.03 ± 0.02	9.44 ± 0.10
^{248}Cm	0.21 ± 0.01	3.33 ± 0.07	3.71 ± 0.07	0.86 ± 0.02	8.11 ± 0.10
^{250}Cf	0.21 ± 0.01	3.27 ± 0.08	3.85 ± 0.08	0.85 ± 0.03	8.18 ± 0.12

(a) From Campbell and McNeilles (ref. 4). Also $I_\gamma(26.35) = 2.44 \pm 0.12/\text{dis}$ and $I_\gamma(59.543) = 35.9 \pm 0.62/\text{dis}$.

Tissue Attenuation and Photon Transport Calculations

Since the most intense photon radiations in the decay of most actinide nuclides are the L-series X rays, it is these radiations that must be observed in external counters. The half-value layer for attenuation by soft tissue for these photons is approximately 0.6 cm and hence severe calibration problems arise. Transmission through bone is negligible and the photons originating in the lung or upper respiratory system must escape the body thru rib interstices. Calibration factors are thus extremely photon energy dependent and are a unique function of the distribution of inhaled particles within the respiratory system.

In an effort to investigate some of the variables which affect external detector calibration factors, we have used Monte Carlo photon transport techniques to calculate the spatial distribution of unattenuated photons that exit the body from various origins within the lung. The Monte Carlo modeling technique is used in conjunction with a mathematical heterogeneous phantom^{(5), (6)} which closely approximates details of the "Reference Man" given in a recent ICRP report⁽⁷⁾ although several simplifying mathematical descriptions are used. As an example, the lung is considered to be one half of an ellipsoid with an anterior section removed. Both lungs are equal in size, 24 cm long and 1689 cm^3 in volume. The photon transport is considered through three different media: lung tissue, soft tissue and bone. The calculations have been carried out for the L_a , L_B , and L_γ lines of the U L-X ray spectrum and for different assumed isotropic point source locations within the volume of the lung and also for the uniform distribution. Those photons that exit the body unattenuated, i.e., have not undergone any collisions, are counted in 0.7 cm x 0.7 cm grid. The distance, 0.7 cm, matches the half distance between ribs and the grid structure is aligned to coincide with the ribs for ease in orientation.

Examples of some of these calculations are given in Tables 3 and 4 where our Monte Carlo calculations have been scaled to match the initial isotropic L-X ray distribution expected from 1 μCi of ^{239}Pu using the absolute group intensities given in Table 2. The calculations given in the Tables are based

Table 3. Calculated ^{239}Pu Point Source Calibration Factors for a 125 cm^2 Detector (Upper 1/3).^(a)

Source Location	$\frac{\text{cpm}}{\mu\text{Ci}}(b)$			
	L_a	L_B	L_γ	zL
Front Surface	3.4	105	104	212.4
Middle	-	12.0	17.9	29.9
Back Surface	-	1.9	4.7	6.6

a. Chest-wall thickness = 3 cm.

b. A useful alternative unit is $\text{cp hour}/\text{MBLB}$ where MBLB = max permissible lung burden = 16 nCi. The conversion factor is $0.96 \times \text{cpm}/\mu\text{Ci} = \text{cp hour}/\text{MBLB}$.

Table 4. Calculated ^{239}Pu Point Source Calibration Factors for a 125 cm^2 Detector (Mid Plane) (a).

Source Location	cpm/ μCi			
	L_α	L_β	L_γ	ΣL
Front Surface	8.7	230	193	431.7
Middle	0.2	16.8	18.8	35.8
Back Surface	-	1.3	2.9	4.2

a. Chest-wall thickness = 2.5 cm.

on point sources located in a vertical plane bisecting the right lung and in a horizontal plane intersecting the upper 1/3 of the lung (Table 3) or in a horizontal plane which bisects the lung (Table 4). Three such point locations are given in each Table for the front surface, middle and back surface of the right lung. The calculated calibration factors are the net counting rates expected in one 125 cm^2 detector, typical for a "Phoswich" scintillation detector, located over the upper portion of the lung.

It is clear from Tables 3 and 4 that soft tissue seriously attenuates the UL-X rays and it is perhaps fortuitous but nonetheless gratifying to note that our calculated calibration factors for the point sources located in the middle of the lung are within the range of values currently used in practice for such detectors. We have also estimated the calibration factors under the same conditions for a 10 cm^2 detector, which represents the state of the art in area for a single spectroscopic grade intrinsic planar Ge detector. For a point source located in the middle of the lung the appropriate calibration factor is $5.4\text{ cpm}/\mu\text{Ci}$, an entirely unexpected result when the relative detector areas are taken into consideration (12.5:1). For the uniform distribution, which is unlikely to be encountered in practice, the relative calibration factors approach the theoretical value of 12.5:1. We are looking forward to improving our modeling techniques to include "realistic" distributions of Pu in the lung that are likely to be encountered in practice.

Conclusions

The application of Ge detectors in the field of in-vivo detection of respired actinides is very promising. Elemental identifications are possible using Ge detectors and using a Ge detector array, determinations of the spatial distribution of the internal emitters are also possible. Clearly, observations of the L-X ray spectra at high resolution with a suitable Ge detector array will lead to more accurate and more sensitive determinations of actinide lung burdens to the benefit of the occupational worker.

References

1. Robertson, R., Spyrou, M. and Kennett, T. J., "Low Level γ -Ray Spectrometry; NaI(Tl) vs Ge(Li) ", Analytical Chemistry 47:65, 1975.
2. O'Kelley, G. D., "The Use of Ge(Li) Detectors in Measurements on Returned Lunar Samples," private communication, June 1975.
3. Benis, C. E., Jr. and Tubbs, L., "Absolute L-Series X-Ray Yields in the Decay of Selected Actinide Nuclides," to be published.
4. Campbell, J. L. and McNelles, L. A., "An Intercomparison of Efficiency-Calibration Techniques for Semiconductor X-Ray Detectors", Nuclear Instruments and Methods 125:205, 1975.
5. Snyder, W. S., Ford, M. R., Warner, G. G. and Fisher, R. L., Jr. "Estimates of Absorbed Fractions for Monoenergetic Photon Sources Uniformly Distributed in Various Organs of a Heterogeneous Phantom," MIRD Pamphlet No. 5, Journal of Nuclear Medicine, Supplement No. 3, 10, 1969.
6. Snyder, W. S., Ford, M. R., Warner, G. G. and Watson, S. B., "A Tabulation of Dose Equivalent per Microcurie-Day for Source and Target Organs of an Adult for Various Radionuclides," Oak Ridge National Laboratory Report, ORNL-5000, Oak Ridge, Tennessee, 1974.
7. Snyder, W. S., Chairman, "Report of the Task Group on Reference Man", ICRP Report No. 23, Pergamon Press, 1975.